Optical Interconnection Architectures based on Microring Resonators

Optical Interconnection Architectures based on Microring Resonators

A. Bianco[1], D. Cuda[1], M. Garrich[2], R. Gaudino[1], G. Gavilanes[1], P. Giaccone[1], F. Neri[1]
1: Politecnico di Torino, ✉ firstname.lastname@polito.it – 2: Universitat Politècnica de Catalunya

Abstract: Microring resonators are an interesting device to build integrated optical interconnects, but their asymmetric loss behavior could limit the scalability of classical optical interconnects. We present new interconnects able to increase scalability with limited complexity.

Keywords: optical interconnects, microring resonators

1. Introduction

The need to carry petabytes of information in high-performance computing systems, and recent breakthroughs in CMOS-compatible silicon photonic are boosting the penetration of optical technologies into interconnection systems. Promising for optical switching are *silicon microring resonators*, small foot-print devices that have been used for filtering, delaying or modulating optical signals. In this paper[a] we first describe some Switching Elements (SE) based on microring resonators. Second, we highlight scalability and complexity limitations of two classical interconnects using microring-based SEs as building blocks. Finally, we propose new hybrid architectures to improve the scalability of microring-based optical interconnects.

2. Microring-based switching elements

Fig 1a illustrates a simple structure of a 1x2 microring-based SE (called 1B-SE). Optical signals entering the *input* port can be deflected either to the *drop* port, when the ring is properly tuned to the input signal wavelength (for instance by carrier injection [1]), or to the *through* port in the normal non-tuned ring state. This 1B-SE presents an asymmetric behavior: experimental measurements [2] show that input signals coupled into the ring suffer larger power losses (due to the propagation inside the ring and the ring-waveguide coupling) than signals routed to the through port. This will also lead to a larger coherent (in-band) crosstalk cumulation in an optical interconnect made of several SEs. Fig. 1b depicts an implementation of a basic 2x2 SE (called 2B-SE) based on two 1B-SEs jointly controlled to provide two switching states: the *bar* state (in1→out1, in2→out2) and the *cross* state (in1→out2, in2→out1). Each ring deflects (lets pass) the corresponding optical input signal to the drop (through) port of the respective 1B-SE when the 2B-SE is configured in the bar (cross) state. Hence, 2B-SE exhibits an asymmetric behavior too: power losses are higher in the bar state, whereas they are negligible in the cross state [3]. In general, we say that microring-based SEs present a High-Loss State (HLS) and a Low-Loss State (LLS). Fig. 1c shows the newly proposed 2x2 Mirrored-SE (called 2M-SE). By cross-connecting input ports, the 2M-SE swaps HLS and LSS with respect to 2B-SE: the bar configuration, corresponding to (in1→out1, in2→out2) is now realized by setting up the internal 2x2 SE in the cross state, whereas the cross state (in1→out2, in2→out1) is achieved with an internal bar state.

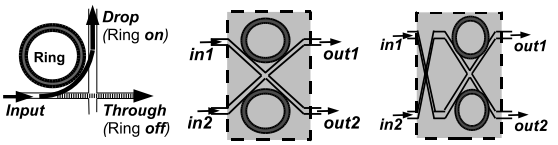

(a) 1x2 Basic SE **(b)** 2x2 Basic SE **(c)** 2x2 Mirrored SE

Fig. 1: Elementary microring-based switching elements

3. Interconnection Architectures

We now study larger (i.e., with more ports) interconnects built as compositions of the above described SEs. For maximum scalability, we aim at minimizing the maximum number of SEs in HLS (either the drop port for a 1B-SE, the bar-state for a 2B-SE, or the cross-state for a 2M-SE) crossed by optical signals for every possible input/output connection. We denote by XC the maximum number of SEs configured in HLS that an input signal must cross in the optical interconnect.

Fig. 2a shows a 4x4 crossbar, based on 1B-SEs; column waveguides are the inputs and row waveguides are the outputs. The crossbar exhibits the best scalability performance, since each input can be connected to any output crossing a single HLS SE (hence $XC = 1$). Despite its optimal scalability performance, the crossbar shows a high complexity, assessed in terms of number of microrings, equal to N^2. As a consequence, it exhibits a large footprint and requires controlling a large number of SEs.

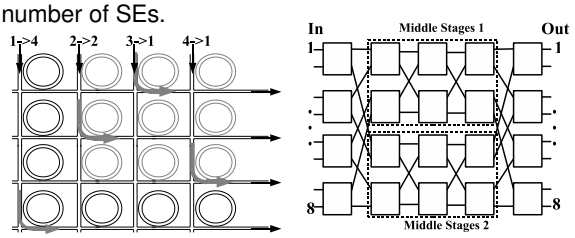

(a) 4x4 microring-based crossbar **(b)** 8x8 Benes network

Fig. 2: Interconnection networks considered

The definition of non-blocking networks less complex than the crossbar naturally leads to multistage interconnects, among which we consider here the Benes network. Benes networks exhibit several advantages, such as a straightforward recursive construction rule, a simple routing and re-arranging algorithm and especially, a complexity (number of crosspoints) asymptotically close to the minimum. Fig. 2b shows a 8x8 Benes network. A $N \times N$ Benes network permits any one-to-one interconnection between inputs and outputs using a number of stages (columns of SEs) equal to $S = 2\log_2 N - 1$, each stage including $N/2$ 2x2 SEs. Hence, the complexity of a $N \times N$ Benes network scales as $\Theta\left(2N \log_2 N\right)$, as each 2x2 SE includes 2 rings. Despite this complexity reduction, $XC = S$ for worst-case

[a]This work was partially supported by the BONE project, a Network of Excellence funded by the European Commission within the 7th Framework Programme.

9781-4244-3856-3/09/$25.00 ©2009 IEEE

paths in a Benes network. Thus, classical multistage architectures don't scale to large port counts because their physical impairments grow with the network depth S.

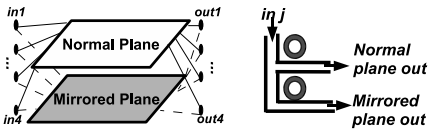

(a) Mirrored architecture **(b)** Plane Selector

Fig. 3: Mirrored architecture and plane selector

To improve scalability of multistage networks (i.e., to reduce XC) we present here the mirroring technique and the new Hybrid Benes-Crossbar (HBC) architecture. The main idea behind the mirroring technique can be illustrated through Fig. 3a. Onto two different spatial planes, we build two interconnection networks which are topologically indistinguishable. On the *normal* plane we build an interconnection architecture based on 2B-SEs, whereas on the *mirrored* plane we deploy the same interconnection network exploiting 2M-SEs. All inputs connect to both planes by means of the plane selector depicted in Fig. 3b (which requires one extra HLS SE). Each output collects information from the two planes by means of a coupler (at a negligible impairments cost with respect to a ring). Exploiting the 2M-SE property of swapping HLS and LLS, all the input/output connections that would cross $K \geq S/2+1$ HLS 2B-SEs in the normal plane can now be routed on the mirrored plane, actually crossing $(S-K)$ HLS 2M-SEs. Thus, by using the mirroring technique, XC reduces to $S/2+1$ instead of S as in the original single-plane architectures.

The HBC solution instead combines the crossbar and the Benes network, and is based on the observation that a $N \times N$ Benes network is made of two edge stages of SEs connected to two $(N/2) \times (N/2)$ non-blocking networks in the middle stage. These non-blocking networks are usually Benes networks as well. However, being crossbars non-blocking and optimal in terms of scalability, they can be employed in the middle stage of a multistage network and then interconnected according to the Benes pattern using edge stages composed by 2x2 SEs. In Fig. 4, four 4x4 crossbars are used as middle stages to build a 16x16 interconnect. These crossbars are firstly employed as building blocks for two 8x8 networks (shaded in Fig. 4), which are then interconnected to build the 16x16 network. The HBC complexity $C_{\text{HBC}}(N,m)$ scales as $\Theta\left(2N\log_2\frac{N}{m}+Nm\right)$, where $2 \leq m \leq N$ is the size of the inner crossbars used in the middle stage ($m=4$ in Fig. 4). Note that, when $m=2$ or $m=N$, the HBC architecture degenerates into a Benes or a crossbar network, respectively. Hence, differently from a Benes network, the HBC architecture is always feasible (by adapting m to the maximum acceptable XC), and presents a constructive rule depending on N and XC: m can be derived from $XC \leq 2\log_2\frac{N}{m}+1$. When mirroring is applied to the HBC architecture (M-HBC), it is possible to show that $m_{\text{M-HBC}} = 2m^2_{\text{HBC}}/N$ with respect to the single plane solution for a given value of XC, and that its complexity scales as $C_{\text{M-HBC}}(N,m) = \Theta\left(2\left(C_{\text{HBC}}(N,2\frac{m^2}{N})+N\right)\right)$.

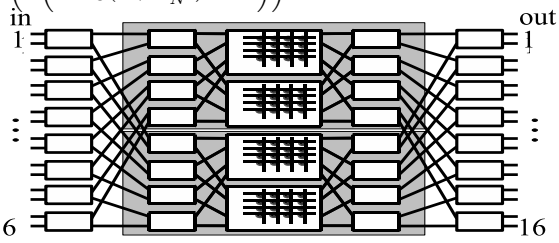

Fig. 4: Hybrid Benes-Crossbar (HBC) network

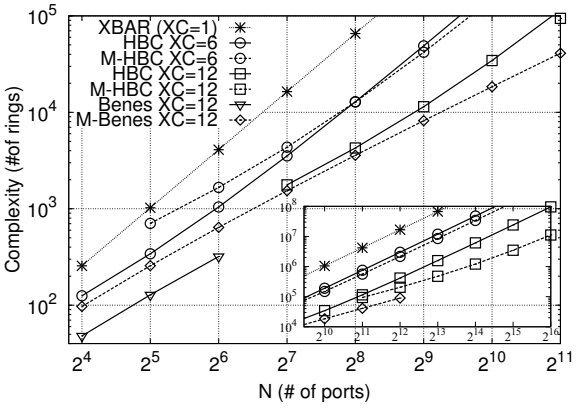

Fig. 5: Complexity and scalability for crossbar, Benes and hybrid Benes-crossbar networks

4. Complexity and scalability

Fig. 5 shows the complexity for the crossbar, the Benes and the HBC networks varying their number of input/output ports N. We considered both single plane (identified by the continuous lines) and mirrored architectures (identified by the "M-" prefixes and by the dashed lines). In addition, we consider $XC=6$ and $XC=12$ to illustrate two feasibility conditions characterized by a maximum of allowed number of crossed HLS SEs which is either quite low or rather high, respectively. m in HBC networks is chosen as to achieve the given XC. The larger figure refers to "small" interconnects (N ranging from 2^4 to 2^{11}), whereas the smaller figure refers to "large" systems (N ranging from 2^{10} to 2^{16}). The Benes network (only shown for $XC=12$) exhibits the lower complexity but also the poorest scalability performance. Exploiting mirroring, the maximum size of a feasible Benes increases from N to N^2 for a given XC. The HBC architecture is always feasible; indeed, appropriately dimensioning m, XC can be upper bounded to $2\log_2\frac{N}{m}+1$. Regarding HBC, mirrored solutions lead to larger complexity for smaller interconnects, whereas mirroring becomes complexity-advantageous when the interconnect size increases. Fig. 5 shows only the M-HBC architectures compliant with the feasibility condition $m_{\text{M-HBC}} \geq 2$. Note that, the smaller XC, the smaller the size of the HBC interconnect for which mirroring becomes complexity-effective.

References

1 C. Li, A.W. Poon, CLEO 2007, Paper JThD115

2 B.G. Lee et al., IEEE Photonic T. L., Vol. 20, Iss. 10, pp. 767-769, May 2008

3 B.G. Lee et al., ECOC 2008, Paper Tu.3.C.3

9781-4244-3856-3/09/$25.00 ©2009 IEEE